# Stabilizing Unstable Flows by Coarse Mesh Observables and Actuators - A Pavement to Data Assimilation

Edriss S. Titi

University of Cambridge
Texas A&M University
and
Weizmann Institute of Science

Conservation Principles, Data, and Uncertainty in Atmosphere-Ocean Modelling

Potsdam, April 2-4, 2019

# Acknowledgements

**Many thanks to the organizers!**

**Collaborators:** D. Albanez, U. Altaf, A. Azouani, H. Bessaih, A. Biswas, A. Celik, A. Farhat, C. Foias, M. Gesho, I. Hoteit, K. Hyden, H. Ibdah, M. Jolly, V. Kalantarov, O. Knio, E. Lunasin, P. Markowich, C. Mondaini, E. Olson, S. Trabelsi.

# The Main Idea: Finitely Many Degrees of Freedom!!

- Conventional theory of turbulence asserts that there are finitely many **"degrees of freedom"** in turbulent flows.
- Instabilities occur in turbulent flows at the large spatial scales, and the viscosity dissipates and stabilizes the fine spatial scales.
- A rigorous mathematical framework, based on dynamical systems approach, was developed to explain this assertion and to identify these **"degrees of freedom"**, such as finite-dimensional attractors, determining modes, determining nodes, etc...
- This dynamical systems approach soon proved to be applicable to a whole class of dissipative evolution equations, such as reaction-diffusion systems, Bénard convection, etc...

# The Main Idea: Finitely Many Degrees of Freedom!!

- Conventional theory of turbulence asserts that there are finitely many **“degrees of freedom”** in turbulent flows.
- Instabilities occur in turbulent flows at the large spatial scales, and the viscosity dissipates and stabilizes the fine spatial scales.
- A rigorous mathematical framework, based on dynamical systems approach, was developed to explain this assertion and to identify these **“degrees of freedom”**, such as finite-dimensional attractors, determining modes, determining nodes, etc...
- This dynamical systems approach soon proved to be applicable to a whole class of dissipative evolution equations, such as reaction-diffusion systems, Bénard convection, etc...

# The Main Idea: Finitely Many Degrees of Freedom!!

- Conventional theory of turbulence asserts that there are finitely many **“degrees of freedom”** in turbulent flows.
- Instabilities occur in turbulent flows at the large spatial scales, and the viscosity dissipates and stabilizes the fine spatial scales.
- A rigorous mathematical framework, based on dynamical systems approach, was developed to explain this assertion and to identify these **“degrees of freedom”**, such as finite-dimensional attractors, determining modes, determining nodes, etc...
- This dynamical systems approach soon proved to be applicable to a whole class of dissipative evolution equations, such as reaction-diffusion systems, Bénard convection, etc...

# The Main Idea: Finitely Many Degrees of Freedom!!

- Conventional theory of turbulence asserts that there are finitely many **"degrees of freedom"** in turbulent flows.
- Instabilities occur in turbulent flows at the large spatial scales, and the viscosity dissipates and stabilizes the fine spatial scales.
- A rigorous mathematical framework, based on dynamical systems approach, was developed to explain this assertion and to identify these **"degrees of freedom"**, such as finite-dimensional attractors, determining modes, determining nodes, etc...
- This dynamical systems approach soon proved to be applicable to a whole class of dissipative evolution equations, such as reaction-diffusion systems, Bénard convection, etc...

# The Question Is:

How can one use these finitely many degrees in real world applications?

- **Data assimilation:** Use the spatial coarse mesh measurements to recover the corresponding unknown reference solutions.
- **Synchronization:** Use partial information on the solution to recover the solution.
- **Control:** Use discrete measurements to stabilize the corresponding unstable system.

# The Question Is:

How can one use these finitely many degrees in real world applications?

- **Data assimilation:** Use the spatial coarse mesh measurements to recover the corresponding unknown reference solutions.
- **Synchronization:** Use partial information on the solution to recover the solution.
- **Control:** Use discrete measurements to stabilize the corresponding unstable system.

# The Question Is:

How can one use these finitely many degrees in real world applications?

- **Data assimilation:** Use the spatial coarse mesh measurements to recover the corresponding unknown reference solutions.
- **Synchronization:** Use partial information on the solution to recover the solution.
- **Control:** Use discrete measurements to stabilize the corresponding unstable system.

# The Question Is:

How can one use these finitely many degrees in real world applications?

- **Data assimilation:** Use the spatial coarse mesh measurements to recover the corresponding unknown reference solutions.
- **Synchronization:** Use partial information on the solution to recover the solution.
- **Control:** Use discrete measurements to stabilize the corresponding unstable system.

# Motivation

- For making a weather forecast, one needs to know the current state of the atmosphere and the Earth's surface.
- *Data assimilation* is used in weather forecasts in order to estimate initial conditions for the forecast model from physical observations.

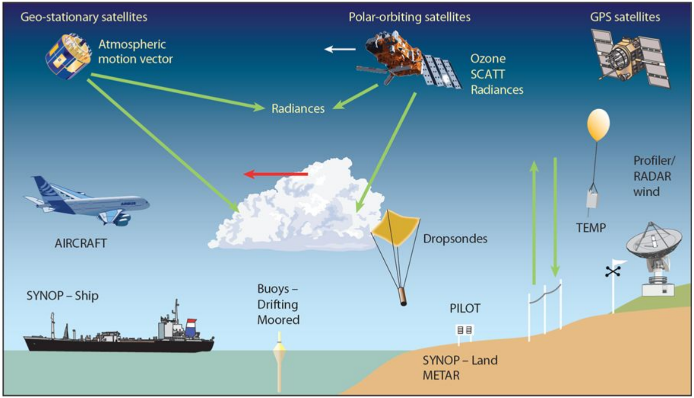


Source: http://www.ecmwf.int

# Data Assimilation

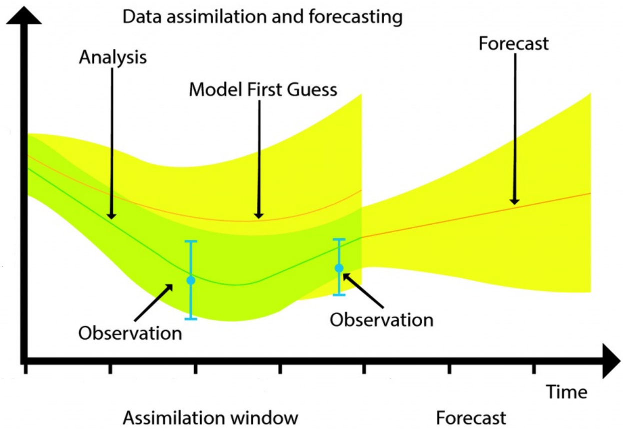

$$\dot{X} = \sigma(Y - X)$$
$$\dot{Y} = \rho X - Y - XZ$$
$$\dot{Z} = XY - \beta Z$$
$$X(0) = X_0,\ Y(0) = Y_0,\ Z(0) = Z_0,$$

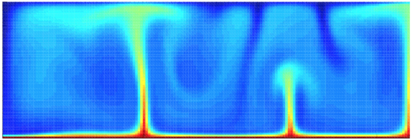


- $X$ - convection roll
- $Y$ - vertical temperature difference
- $Z$ - horizontal temperature difference

- Parameters
  - $\rho = \dfrac{Ra}{Ra_c}$
  - $\beta = \dfrac{\text{Char lengthscale}}{\text{distance b/w 2 plates}}$
  - $\sigma = \dfrac{\nu}{\kappa} = \dfrac{\text{viscosity}}{\text{thermal diff}}$

# Lorenz System

$$\dot{X} = \sigma(Y - X)$$
$$\dot{Y} = \rho X - Y - XZ$$
$$\dot{Z} = XY - \beta Z$$
$$X(0) = X_0,\ Y(0) = Y_0,\ Z(0) = Z_0,$$

Thermal convection, constant viscosity

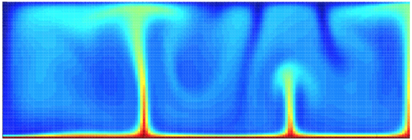

- $X$ - convection roll
- $Y$ - vertical temperature difference
- $Z$ - horizontal temperature difference
- Parameters
  - $\rho = \frac{Ra}{Ra_c}$
  - $\beta = \frac{\text{Char lengthscale}}{\text{distance b/w 2 plates}}$
  - $\sigma = \frac{\nu}{\kappa} = \frac{\text{viscosity}}{\text{thermal diff}}$

# Properties of Lorenz System

- The system is dissipative, i.e., the solution are asymptotically bounded independent of the initial data:

**Theorem**

*Let $(X(t), Y(t), Z(t))$ be the solution to the Lorenz system starting from the initial data $(X_0, Y_0, Z_0)$. Let $\beta > 1$, and define*

$$\overline{K} = 2\left(\frac{\beta(\rho+\sigma)}{\sqrt{2}\mu(\beta-1)}\right) + 3(\sigma+\rho)^2,$$

*where $\mu = \min(1, \sigma)$. Then, there exists a finite time $t_0^* = t_0^*(X_0, Y_0, Z_0, \beta, \rho, \sigma) > 0$ such that*

$$|(X(t), Y(t), Z(t))|^2 \leq \overline{K}, \quad \text{for all} \quad t \geq t_0^*.$$

.

# Properties of Lorenz System

- The system is dissipative, i.e., the solution are asymptotically bounded independent of the initial data:

**Theorem**

*Let $(X(t), Y(t), Z(t))$ be the solution to the Lorenz system starting from the initial data $(X_0, Y_0, Z_0)$. Let $\beta > 1$, and define*

$$\overline{K} = 2\left(\frac{\beta(\rho+\sigma)}{\sqrt{2}\mu(\beta-1)}\right) + 3(\sigma+\rho)^2,$$

*where $\mu = \min(1,\sigma)$. Then, there exists a finite time $t_0^* = t_0^*(X_0, Y_0, Z_0, \beta, \rho, \sigma) > 0$ such that*

$$|(X(t), Y(t), Z(t))|^2 \leq \overline{K}, \quad \textit{for all} \quad t \geq t_0^*.$$

.

# Properties of Lorenz System

Chaotic, sensitive to initial conditions: Check out a YOUTUBE VIDEO.

## Properties of Lorenz System

- Chaotic, sensitive to initial conditions:
  - $\sigma = 10,\ \rho = 28,\ \beta = \frac{8}{3}, \quad (X_0, Y_0, Z_0), \quad (X_0 + 10^{-3}, Y_0, Z_0)$

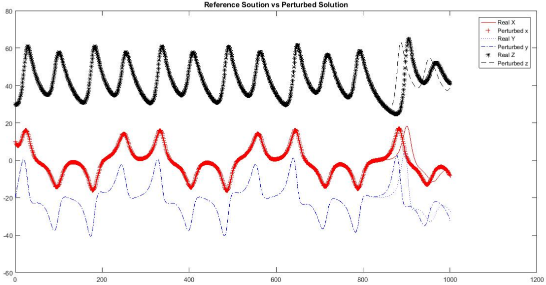


Figure: $X(t), Y(t), Z(t)$ vs. time(units of $\Delta t$)

# Synchronization

Synchronization between two dynamical systems starting with different initial conditions implies that the trajectory of one system converges to the trajectory of the other system.

- Question: Is it possible to synchronize two chaotic systems starting with different initial conditions?
- Answer: Yes! (For Dissipative Systems).
- By some sort of data assimilation.
- A quick demo for the overview of result

# Synchronization

Synchronization between two dynamical systems starting with different initial conditions implies that the trajectory of one system converges to the trajectory of the other system.

- Question: Is it possible to synchronize two chaotic systems starting with different initial conditions?
- Answer: Yes! (For Dissipative Systems).
- By some sort of data assimilation.
- A quick demo for the overview of result

# Synchronization

Synchronization between two dynamical systems starting with different initial conditions implies that the trajectory of one system converges to the trajectory of the other system.

- Question: Is it possible to synchronize two chaotic systems starting with different initial conditions?
- Answer: Yes! (For Dissipative Systems).
- By some sort of data assimilation.
- A quick demo for the overview of result

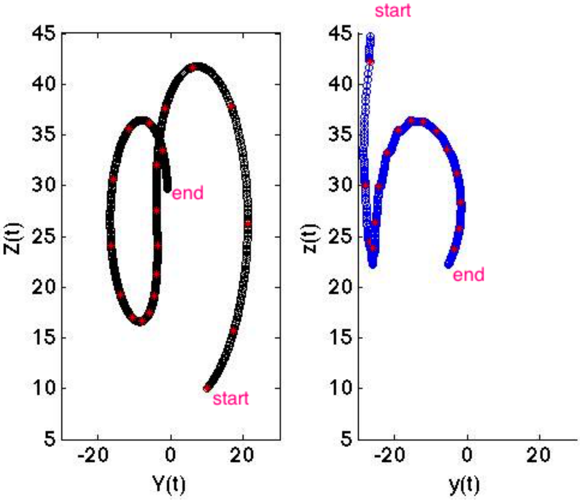
start
end
45
40
35
30
25
20
15
10
5
-20
0
20
Y(t)
Z(t)
y(t)
z(t)

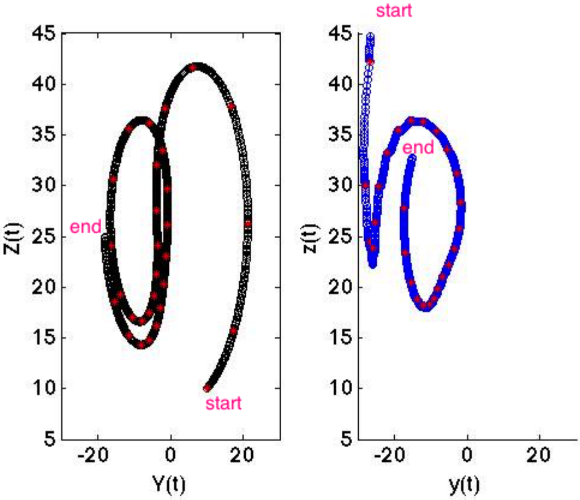

45
40
35
30
25
20
15
10
5
Z(t)
end
start
-20
0
20
Y(t)
start
45
40
35
30
25
20
15
10
5
z(t)
end
-20
0
20
y(t)

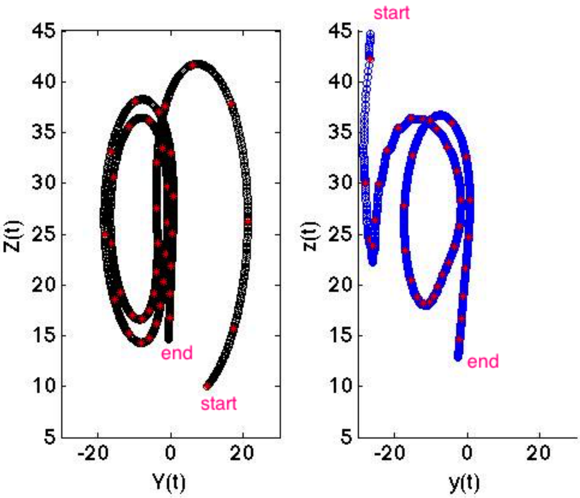
45
40
35
30
25
20
15
10
5
Z(t)
-20
0
20
Y(t)
end
start
start
45
40
35
30
25
20
15
10
5
z(t)
-20
0
20
y(t)
end

# Synchronization of two Lorenz systems

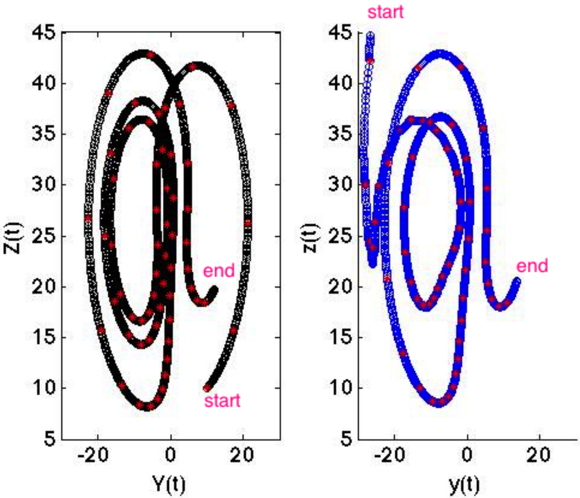

# Results

- Indeed one can show the validity of certain data assimilation algorithms applied to the Lorenz Equations
- Show analytically and numerically that the proposed algorithms allow for the synchronization of the two chaotic systems.

# Application

- Atmospheric Applications: data assimilation algorithms, where some state variable observations are not available as an input have been used for simplified numerical hydrodynamic forecast models.
- Numerical experiment of Charney in 1969 confirms that wind and surface pressure can be determined from coarse mesh measurements of temperatures alone.

# Algorithms - Direct Insertion - Continuous case

- Direct Insertion (Continuous case) - observational measurements from a known reference solution are directly inserted into the evolution equation of the slaved system.
  - Coupling on X ☑
  - Coupling on Y ☑
  - Coupling on Z
- Direct Insertion Discrete case - Data is inserted into the slaved system only at specific times.
  - Coupling on X ☑
  - Coupling on Y ☑

# Direct Insertion (DI) Coupling on X

- partial observational measurements from a known **reference solution** are directly inserted into the evolution equation of the slaved system.

$$\begin{cases} \dot{X} = -\sigma X + \sigma Y, & X(0) = X_0 \\ \dot{Y} = \rho X - Y - XZ, & Y(0) = Y_0 \\ \dot{Z} = XY - \beta Z, & Z(0) = Z_0 \\ \dot{y} = \rho X - y - Xz, & y(0) = y_0 \\ \dot{z} = Xy - \beta z, & z(0) = z_0 \end{cases} \tag{1}$$

$x(t) = X(t)$, $y_0 \neq Y_0$ and $z_0 \neq Z_0$

# Direct Insertion (DI) Coupling on X

- partial observational measurements from a known **reference solution** are directly inserted into the evolution equation of the slaved system.

$$\begin{cases} \dot{X} = -\sigma X + \sigma Y, & X(0) = X_0 \\ \dot{Y} = \rho X - Y - XZ, & Y(0) = Y_0 \\ \dot{Z} = XY - \beta Z, & Z(0) = Z_0 \\ \dot{y} = \rho X - y - Xz, & y(0) = y_0 \\ \dot{z} = Xy - \beta z, & z(0) = z_0 \end{cases} \tag{1}$$

$x(t) = X(t)$, $y_0 \neq Y_0$ and $z_0 \neq Z_0$

# Direct Insertion Coupling on Y

- partial observational measurements from a known **reference solution** are directly inserted into the evolution equation of the slaved system.

$$\begin{cases} \dot{X} = -\sigma X + \sigma Y, & X(0) = X_0 \\ \dot{Y} = \rho X - Y - XZ, & Y(0) = Y_0 \\ \dot{Z} = XY - \beta Z, & Z(0) = Z_0 \\ \dot{x} = \sigma(Y - x), & x(0) = x_0 \\ \dot{z} = xY - \beta z, & z(0) = z_0 \end{cases} \tag{2}$$

# Direct Insertion Algorithm Coupling on Z

- a crucial example where direct insertion in only one state variable does not allow for synchronization

$$\begin{cases} \dot{X} = -\sigma X + \sigma Y, & X(0) = X_0 \\ \dot{Y} = \rho X - Y - XZ, & Y(0) = Y_0 \\ \dot{Z} = XY - \beta Z, & Z(0) = Z_0 \\ \dot{x} = \sigma(y - x), & x(0) = x_0 \\ \dot{y} = \rho x - y - xZ, & y(0) = y_0 \end{cases} \tag{3}$$

Interpretation: continuous measurements on the horizontal temperature difference $(Z(t))$ is not enough to determine the full state of the system.

# Numerics DI Coupling on X

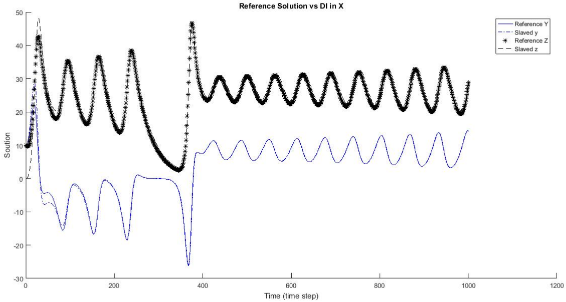

# Numerics DI Coupling on Y

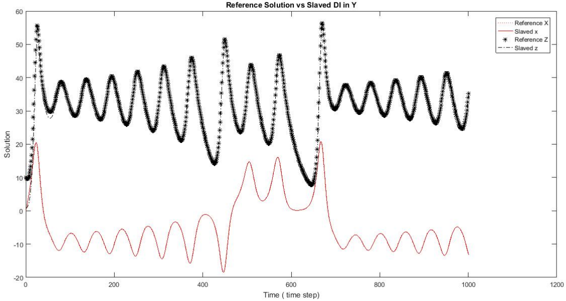


Plot of $x, X, z, Z$ vs time step with DI on $Y$.:
$\sigma = 10, \rho = 28, \beta = \frac{8}{3}$, $IC_{reference} = [0, 10, 10]$, $IC_{slaved} = [1, 0, 1]$,
$t = [0, 10]$ and $\Delta t = \frac{1}{100}$.

# Coupling in $X$ - steady states

Set $\rho > 1$ : Stationary points for the Lorenz system:
$(X, Y, Z) = \left(\pm\sqrt{\beta(\rho-1)}, \pm\sqrt{\beta(\rho-1)}, \rho-1\right)$

- Stationary points for the coupled system: (Coupling in $X$.)
- Set $\dot{X} = \dot{Y} = \dot{Z} = \dot{y} = \dot{z} = 0$.
- The master equation have similar stationary points as above.
- For the slaved system:
  $0 = \dot{y} = \rho X - y - Xz, \quad 0 = \dot{z} = Xy - \beta z.$
- $y = X(\rho - z) = \pm\sqrt{\beta(\rho-1)}(\rho - z) \quad z = \dfrac{Xy}{\beta}.$
- Solving by substitution: $y = \pm\sqrt{\beta(\rho-1)}, \quad \rho - 1.$
- Conclusion: $y = Y$, $z = Z$. $1-1$ correspondence with the stationary points of the master equation.

# Coupling in $X$ - steady states

Set $\rho > 1$ : Stationary points for the Lorenz system:
$(X, Y, Z) = \left(\pm\sqrt{\beta(\rho-1)}, \pm\sqrt{\beta(\rho-1)}, \rho - 1\right)$

- Stationary points for the coupled system: (Coupling in $X$.)
- Set $\dot{X} = \dot{Y} = \dot{Z} = \dot{y} = \dot{z} = 0$.
- The master equation have similar stationary points as above.
- For the slaved system:
  $0 = \dot{y} = \rho X - y - Xz, \quad 0 = \dot{z} = Xy - \beta z.$
- $y = X(\rho - z) = \pm\sqrt{\beta(\rho-1)}(\rho - z) \quad z = \dfrac{Xy}{\beta}.$
- Solving by substitution: $y = \pm\sqrt{\beta(\rho-1)}, \quad \rho - 1.$
- Conclusion: $y = Y$, $z = Z$. $1-1$ correspondence with the stationary points of the master equation.

# Coupling in $Y$ - steady states

Set $\rho > 1$ : Stationary points for the Lorenz system:
$(X, Y, Z) = \left(\pm\sqrt{\beta(\rho-1)}, \pm\sqrt{\beta(\rho-1)}, \rho - 1\right)$

- Stationary points for the coupled system: (Coupling in $Y$.)
- Set $\dot{X} = \dot{Y} = \dot{Z} = \dot{x} = \dot{z} = 0$.
- The master equation have similar stationary points as above.
- For the slaved system:

  $$x = Y = \pm\sqrt{\beta(\rho-1)} \quad z = \frac{xY}{\beta} = \rho - 1.$$

- $x = X(\rho - z) = \pm\sqrt{\beta(\rho-1)}(\rho - z) \quad z = \dfrac{Xy}{\beta}$.
- Conclusion: $x = X$, $z = Z$. 1-1 correspondence with the stationary points of the master equation.

# Coupling in $Y$ - steady states

Set $\rho > 1$ : Stationary points for the Lorenz system:
$(X, Y, Z) = \left(\pm\sqrt{\beta(\rho-1)}, \pm\sqrt{\beta(\rho-1)}, \rho - 1\right)$

- Stationary points for the coupled system: (Coupling in $Y$.)
- Set $\dot{X} = \dot{Y} = \dot{Z} = \dot{x} = \dot{z} = 0$.
- The master equation have similar stationary points as above.
- For the slaved system:

  $$x = Y = \pm\sqrt{\beta(\rho-1)} \quad z = \frac{xY}{\beta} = \rho - 1.$$

- $x = X(\rho - z) = \pm\sqrt{\beta(\rho-1)}(\rho - z) \quad z = \dfrac{Xy}{\beta}$.
- Conclusion: $x = X$, $z = Z$. 1-1 correspondence with the stationary points of the master equation.

# Coupling in $Z$ - Non-matching steady states

$$\begin{cases} 0 = \dot{X} = -\sigma X + \sigma Y, & X(0) = X_0 \\ 0 = \dot{Y} = \rho X - Y - XZ, & Y(0) = Y_0 \\ 0 = \dot{Z} = XY - \beta Z, & Z(0) = Z_0 \\ 0 = \dot{x} = \sigma(y - x), & x(0) = x_0 \\ 0 = \dot{y} = \rho x - y - xZ, & y(0) = y_0 \end{cases} \tag{4}$$

For the last two equations $x = y$ and $y(z - \rho + 1) = 0$. But $Z = \rho - 1$ so $y$ can be arbitrary.
We get infinitely many stationary points:
$(X, Y, Z, x, y) = \left(\pm\sqrt{\beta(\rho - 1)}, \pm\sqrt{\beta(\rho - 1)}, \rho - 1, x, y\right)$
[Ref: Hayden, 2006)]

# Numerics DI Coupling on Z - NO SYNCHRONIZATION

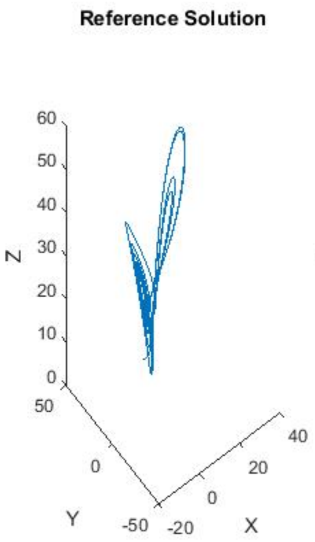


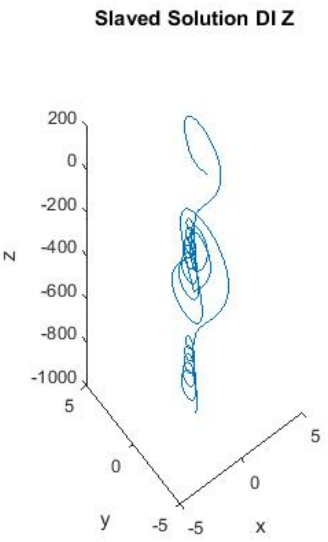

# DI Coupling on X Theorem - Convergence Theorem

**Theorem**

*Let* $\beta > 1$. *Let* $(X(t), Y(t), Z(t), y(t), z(t))$ *be the solution to the system* (1). *Then* $|Y - y| \to 0$, *and* $|Z - z| \to 0$ *exponentially as* $t \to \infty$.

- Ideal situation: observational data $X(t)$ is known continuously for all times.
- *Why it works:* if $X(t)$ for the system (1) is known for all $t \geq 0$,

$$\begin{cases} \dot{X} = -\sigma X + \sigma Y, & X(0) = X_0 \\ \dot{Y} = \rho X - Y - XZ, & Y(0) = Y_0 \\ \dot{Z} = XY - \beta Z, & Z(0) = Z_0 \end{cases} \tag{5}$$

- In physical applications, measurements are contaminated with errors and thus $\dot{X}$ cannot be properly computed.
- Observational measurements are generally known only at discrete times.

# Convergence - Coupling in the $X$ state variable

**Theorem**

*Let $\beta > 1$. Suppose $(X_1, Y_1, Z_1)(t)$ and $(X_2, Y_2, Z_2)(t)$ are two solutions to the Lorenz system (1) such that $|X_1 - X_2| \to 0$ as $t \to \infty$. Then $|Y_1 - Y_2| \to 0$ and $|Z_1 - Z_2| \to 0$ as $t \to \infty$.*

# Direct Insertion - Discrete Coupling on X

Data is known for $X(t)$ only at certain times $t_0 < t_1 < t_2, \cdots < t_i < t_N$, $|t_i - t_j| = h$ for $j \neq i$. Evolve both systems and reinitialize the slaved system when $X(t_i)$ data is known.

$$\begin{cases} \dot{X} = -\sigma X + \sigma Y, & X(0) = X_0 \\ \dot{Y} = \rho X - Y - XZ, & Y(0) = Y_0 \\ \dot{Z} = XY - \beta Z, & Z(0) = Z_0 \\ \dot{x} = \sigma(y - x), & x(0) = X(0) \\ \dot{y} = \rho x - y - xz, & y(0) = y_0 \\ \dot{z} = xy - \beta z, & z(0) = z_0 \end{cases} \tag{6}$$

# Direct Insertion Discrete Coupling on X

Note: The distance $h$ between observations is crucial to the synchronization of the slaved system to the master equations.
Analysis: Sufficient condition on the size of $h$ to achieve synchronization is done by Hayden-Olson-Titi in [4].

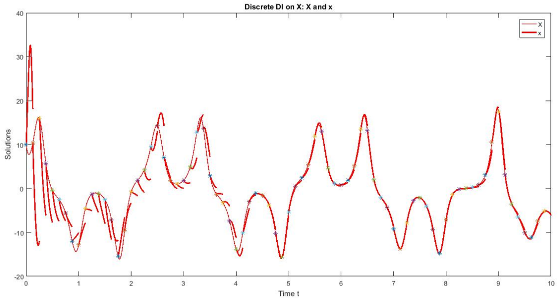


Plot of $X$ and $x$ vs time for the discrete DI on $X$:
$\sigma = 10, \rho = 28, \beta = \frac{8}{3}$, $IC_{reference} = [0, 10, 10]$,
$IC_{slaved} = [10, 45, -15]$, $t = 10$, 80 observations, $h = .125$.

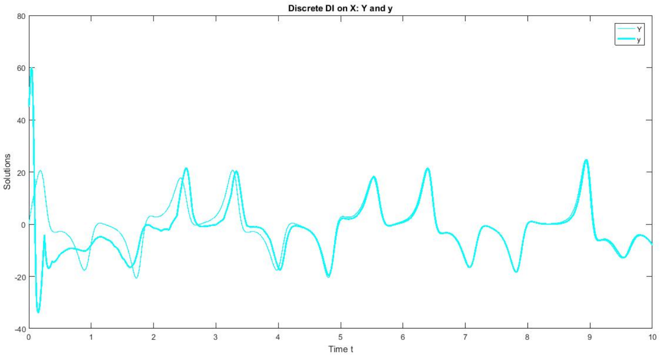


Plot of $Y$ and $y$ vs time for the discrete DI on $X$:
$\sigma = 10, \rho = 28, \beta = \frac{8}{3}$, $IC_{reference} = [0, 10, 10]$,
$IC_{slaved} = [10, 45, -15]$, $t = 10$, 80 observations, $h = .125$.

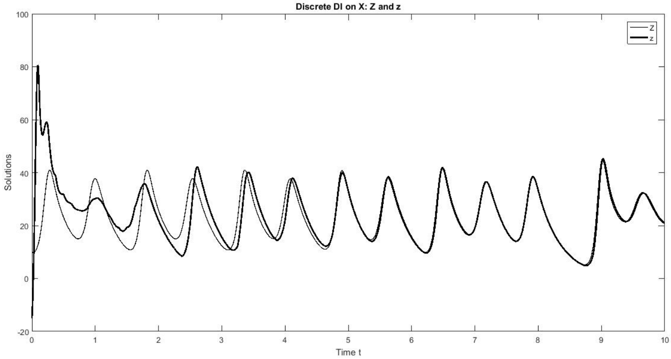


Plot of $Z$ and $z$ vs time for the discrete DI on $X$:
$\sigma = 10, \rho = 28, \beta = \frac{8}{3}$, $IC_{reference} = [0, 10, 10]$,
$IC_{slaved} = [10, 45, -15]$, $t = 10$, 80 observations, $h = .125$.

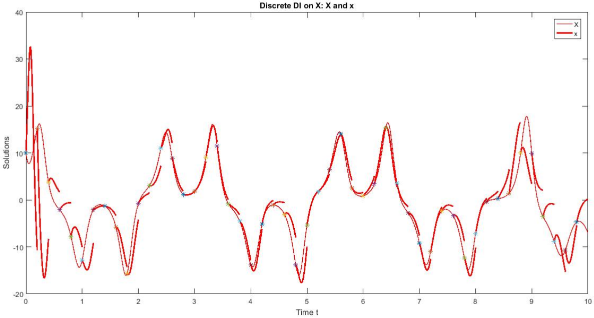


Plot of $X$ vs time for both the reference and slaved solution with discrete DI on $X$: $\sigma = 10, \rho = 28, \beta = \frac{8}{3}$, $IC_{reference} = [0, 10, 10]$, $IC_{slaved} = [10, 45, -15]$, $t = 10$, 50 observations, $h = .2$.

# Non-synchronization with fewer data

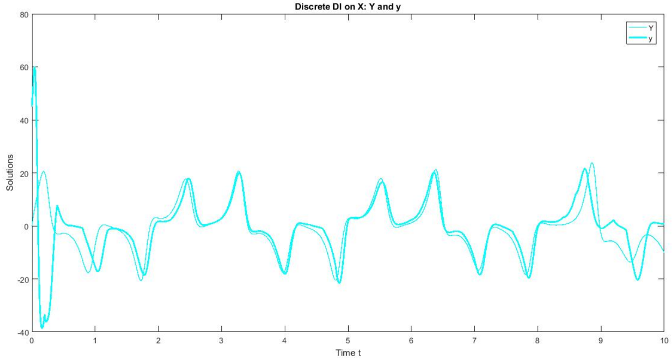


Plot of $Y$ vs time for both the reference and slaved solution with discrete DI on $X$: $\sigma = 10, \rho = 28, \beta = \frac{8}{3}$, 50 observations, $h = .2$.

# Non-synchronization with fewer data

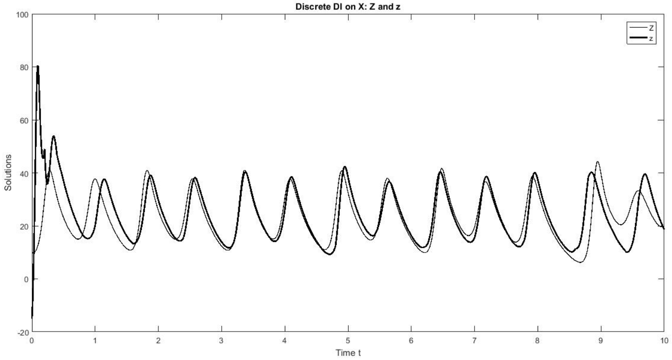


Plot of $X$ vs time for both the reference and slaved solution with discrete DI on $X$. $\sigma = 10, \rho = 28, \beta = \frac{8}{3}$, 50 observations, $h = .2$.

- Direct Insertion (Continuous) - observational measurements from a known reference solution are directly inserted into the evolution equation of the slaved system.
  - Coupling on X ☑
  - Coupling on Y ☑
  - Coupling on Z [No using Direct Insertion, but YES using Newtonian Relaxation scheme]
- Direct Insertion Discrete ($h$ small enough)
  - Coupling on X ☑
  - Coupling on Y ☑

# Newtonian Relaxation: Continuous coupling on $Z$

Lorenz system with continuous coupling on the $Z$ variable using Newtonian relaxation

$$\begin{cases} \dot{X} = -\sigma X + \sigma Y, & X(0) = X_0 \\ \dot{Y} = \rho X - Y - XZ, & Y(0) = Y_0 \\ \dot{Z} = XY - \beta Z, & Z(0) = Z_0 \\ \dot{x} = \sigma(y - x), & x(0) = x_0 \\ \dot{y} = \rho x - y - xz, & y(0) = y_0 \\ \dot{z} = xy - \beta z + \mu_3(Z - z), & z(0) = z_0 \end{cases} \tag{7}$$

where $\mu_3 > 0$, $x(0) = x_0$, $y(0) = y_0$, $z(0) = z_0$ and generally $x_0 \neq X_0$, $y(0) \neq Y_0$, $z(0) \neq Z_0$.

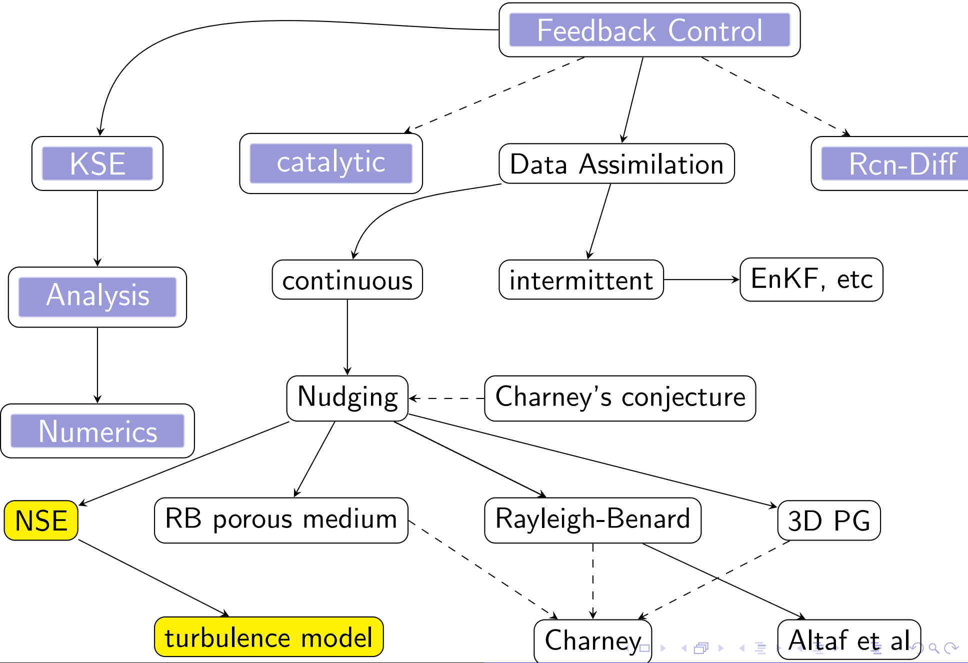
Feedback Control
KSE
catalytic
Data Assimilation
Rcn-Diff
Analysis
continuous
intermittent
EnKF, etc
Numerics
Nudging
Charney's conjecture
NSE
RB porous medium
Rayleigh-Benard
3D PG
turbulence model
Charney
Altaf et al

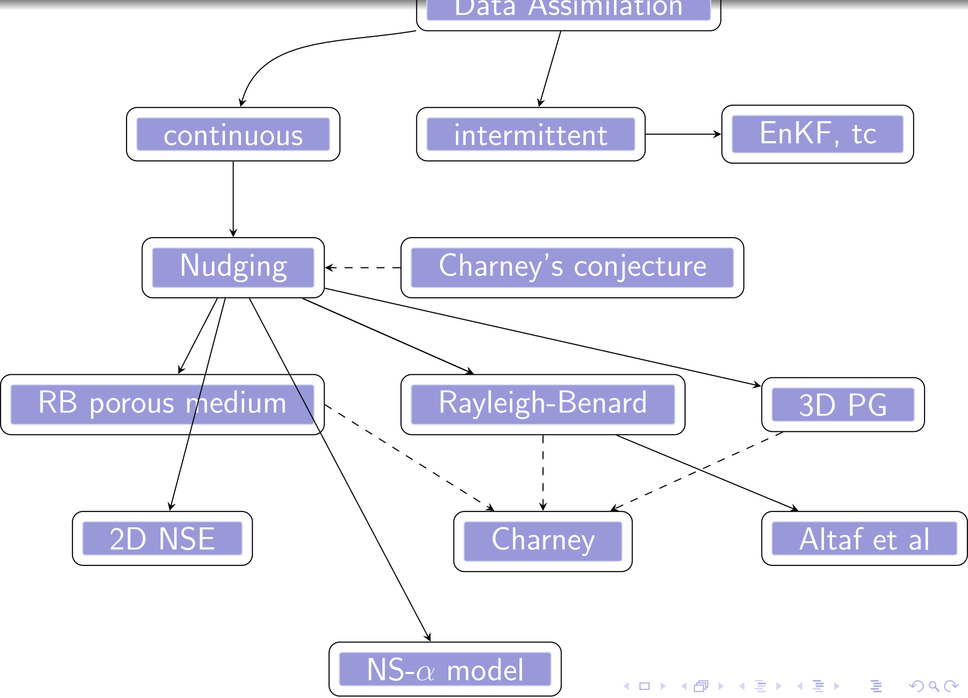
Data Assimilation
continuous
intermittent
EnKF, tc
Nudging
Charney's conjecture
RB porous medium
Rayleigh-Benard
3D PG
2D NSE
Charney
Altaf et al
NS-$\alpha$ model

# Efficient Algorithms

Control and stabilization of flows for various chemical processes or any transport-reaction-diffusion systems

- **rapid thermal chemical vapor deposition** – to produce thin films coatings for surfaces for defense-related applications
- **catalytic rod reactor, tubular reactor** - require reactor temperature to not exceed a certain value, or require a product concentration to not drop below some purity requirement

Ref: Nonlinear and Robust Control of PDE Systems [by Christofides].

Ref: Control and Optimization of Multiscale Process Systems, [by Christofides, Armaou, Lou, Varshney]

# Finite degrees of freedom

- The model equations are known to have a finite number of degrees of freedom.
- **Early attempts:** feedback control approaches are based on reduced order models. (Ahuja2009, Christofides2000,Christofides2003, Foias-Jolly-Kevrekidis-Sell-Titi 88, Jolly-Kevrekidis-Titi 90, Shvartsman-Theodoropolous, Rico-Martinez - Titi - Mounziares 2000)
- analytical work in feedback control theory justifying these algorithms.
- Set-back on the real time implementation of these algorithms in industrial control systems.

# Introduction

- Feedback control scheme by Azouani and Titi 2013 - allows for general observations rather than just Fourier modes, uses finitely many observables and controllers. Some concurrent work by Bloemker et al, (2013), Law et al (2013) - spectral case, data contains noise.
- For systems that possess finite number of determining parameters or degrees of freedom.
- Example: finite number of determining Fourier modes, determining nodes, and determining interpolants and projections.

# Introduction

- Applications to new **continuous data assimilations algorithm** (observational data measurements are free of noise) and **signal synchronization** (recover the soln of the underlying dissipative system from the transmitted partial data). (Azouani-Olson-Titi-2003, Farhat-Jolly-Titi14, Farhat-Lunasin-Titi 2014,15,16, Markowich-Titi-Trabelsi15 )
- Goal: Use low spatial resolution obs. measurements to find reference soln.
- Feedback control algorithm applied to data assimilations where the observational data contains stochastic noise (Bessaih-Olson-Titi 2014).

\- E(approximate solution - exact solution)

$$\leq \text{f(Grashof)} * \text{variance of noise},$$

- Applications to new **continuous data assimilations algorithm** (observational data measurements are free of noise) and **signal synchronization** (recover the soln of the underlying dissipative system from the transmitted partial data). (Azouani-Olson-Titi-2003, Farhat-Jolly-Titi14, Farhat-Lunasin-Titi 2014,15,16, Markowich-Titi-Trabelsi15 )
- Goal: Use low spatial resolution obs. measurements to find reference soln.
- Feedback control algorithm applied to data assimilations where the observational data contains stochastic noise (Bessaih-Olson-Titi 2014).

- E(approximate solution - exact solution)

$\leq$ f(Grashof) * variance of noise,

# Chafee-Infante equations: Finite volume elements

- Feedback control scheme to stabilize the steady state solution $\mathbf{v} \equiv 0$:

$$\frac{\partial u}{\partial t} - \nu\, u_{xx} - \alpha u + u^3 = -\mu \sum_{k=1}^{N} \overline{u}_k\, \chi_{J_k}(x), \tag{8}$$

$$u_x(0) = u_x(L) = 0, \tag{9}$$

- $J_k = \left[(k-1)\frac{L}{N}, k\frac{L}{N}\right)$, for $k = 1, \dots, N-1$, and $J_N = \left[(N-1)\frac{L}{N}, L\right]$,
- $\chi_{J_k}(x)$ is the characteristic function of the interval $J_k$, for $k = 1, \dots, N$, serving as the actuator shape function,
- $$\bar{\varphi}_k = \frac{1}{|J_k|} \int_{J_k} \varphi(x)\, dx = \frac{N}{L} \int_{J_k} \varphi(x)\, dx,$$

  represents the amplitude for the given actuator.
- local averages of the solution, $\overline{u}_k$, for $k = 1, \dots, N$, are the observables, and serve as feedback controllers in (8).

AzTi2013 showed that every solution $u$ of (8)-(9) tends to zero, as $t \to \infty$, under specific explicit assumptions on $N$, in terms of the physical parameters $\nu, \alpha, L$ and $\mu$.

# Kuramoto-Sivashinsky equation (Lunasin, Titi 2016)-

(a model for thin-film flows)
In one dimensional it is written as

$$\frac{\partial u}{\partial t} = -\gamma \frac{\partial^2 u}{\partial x^2} - \nu \frac{\partial^4 u}{\partial x^4} - u \frac{\partial u}{\partial x}, \quad x \in [0, L] \tag{10}$$

subject to the periodic boundary conditions, and initial condition:

$$u(x, 0) = u_0(x), \tag{11}$$

where $u(x, t)$ denotes the height of the film, and the parameters $\gamma$ and $\nu$ are given positive constants. Equation (10) can be nondimensionalized by substituting $u \to \gamma u/\tilde{L}$, $t \to t\tilde{L}^2/\gamma$, $x \to \tilde{L}x$, and $\nu \to \tilde{L}^2\gamma\nu$, with $\tilde{L} = \dfrac{L}{2\pi}$ In this case one gets the same equation as before with the modification $\gamma = 1$ and $L = 2\pi$.

# Terms

- $\dfrac{\partial^2 u}{\partial x^2}$ - responsible for internal destabilizing of the system
- $\dfrac{\partial^4 u}{\partial x^4}$ - responsible for dissipating energy and stabilizes the system.
- $u\dfrac{\partial u}{\partial x}$ transfers energy from low modes to high modes.

# KSE, $\nu < 1$

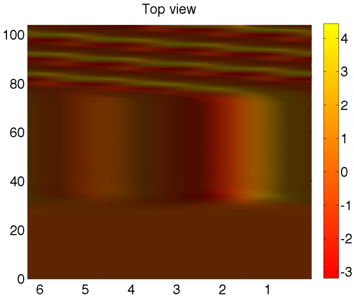


- Case ($\nu = 4/15 < 1$) : thin film flowing in an inclined surface exhibits unwanted wavy fluctuations.
- At around time $t = 32$ a pattern starts to evolve.

# Finding the number of feedback controllers

- Linearize equation (10) about $\mathbf{v} \equiv 0$, subject to periodic boundary conditions,

$$\frac{\partial \mathbf{v}}{\partial t} = -\frac{\partial^2 \mathbf{v}}{\partial x^2} - \nu \frac{\partial^4 \mathbf{v}}{\partial x^4}, \quad x \in [0, 2\pi], \tag{12}$$

- Ansatz: $\mathbf{v}(x,t) = a_k(t)\, e^{ikx}$ that yields the equation

$$\dot{a_k} = (k^2 - \nu k^4) a_k, \tag{13}$$

- solution, with initial condition $\mathbf{v}_0(x) = A_k e^{ikx}$, with $A_k \in \mathbb{R}$,

$$a_k(t) = A_k\, e^{k^2(1-\nu k^2)t}$$

# Number of Unstable modes

$$a_k(t) = A_k \, e^{k^2(1-\nu k^2)t}$$

Conclusion:

- the solution have a range of unstable wave numbers $k < \frac{1}{\sqrt{\nu}}$.
- one needs at least $\frac{1}{\sqrt{\nu}}$ number of parameters to stabilize $\mathbf{v} \equiv 0$.
- the nonlinear system (10), is locally unstable when $\nu < 1$.

as soon as $\nu$ decreases below one atleast one Fourier freq. becomes unstable in the linearized model.

# Number of Unstable modes

$$a_k(t) = A_k\, e^{k^2(1-\nu k^2)t}$$

Conclusion:

- the solution have a range of unstable wave numbers $k < \frac{1}{\sqrt{\nu}}$.
- one needs at least $\frac{1}{\sqrt{\nu}}$ number of parameters to stabilize $\mathbf{v} \equiv 0$.
- the nonlinear system (10), is locally unstable when $\nu < 1$.

as soon as $\nu$ decreases below one atleast one Fourier freq. becomes unstable in the linearized model.

# Case 0: KSE without feedback control, $\nu < 1$

- proof-of-concept: $\nu > 1$ vs. $\nu < 1$
- Initial condition: $1e^{-10} * \cos x \, (1 + \sin x)$ for both of the cases.
- Case: $(\nu = 1.1 > 1)$, linear stability analysis shows exponential decay to the linearly stable steady state zero solution.

# Case when $\nu > 1$

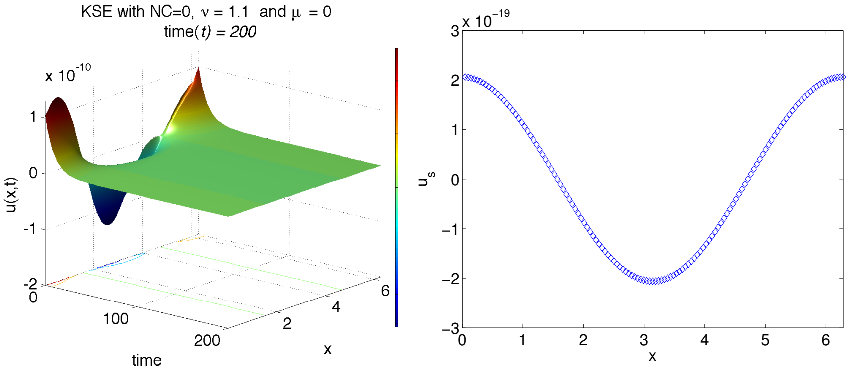


Figure: (a) Open-loop profile showing stability of the $u(x,t) = 0$ steady state solution when $\nu = 1.1 > 1$ (b) Profile of $u(x, t = 200)$.

# Case when $\nu < 1$

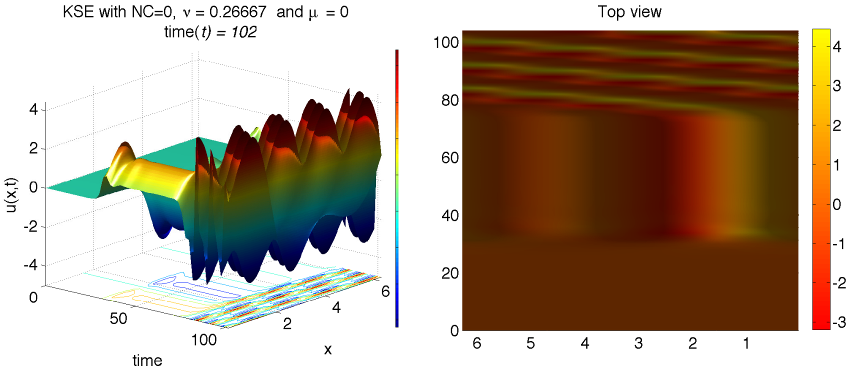


Figure: (a) Open-loop profile showing instability of the $u(x, t) = 0$ steady state solution when $\nu = 4/15 < 1$. (b) Top view profile of $u(x, t)$

# Case 0: KSE without feedback control, $\nu < 1$

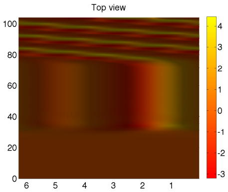


- Case ($\nu = 4/15 < 1$) : experimentally observed that a thin film flowing in an inclined surface exhibits unwanted wavy fluctuations.
- At around time $t = 32$ a pattern starts to evolve.
- Main goal: [Christofides et al [2001+], Ahuja[2009]]. A control strategy to suppress the undesirable occurrences of these wavy patterns by using actuators/sensors that controls the thin film's thickness
- Design a control algorithm that can be achieved **in real time** making the implementation tractable for industrial control system problems.

# Case 0: KSE without feedback control, $\nu < 1$

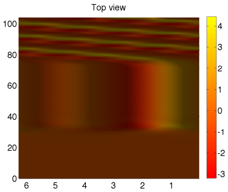


- Case ($\nu = 4/15 < 1$) : experimentally observed that a thin film flowing in an inclined surface exhibits unwanted wavy fluctuations.
- At around time $t = 32$ a pattern starts to evolve.
- Main goal: [Christofides et al [2001+], Ahuja[2009]]. A control strategy to suppress the undesirable occurrences of these wavy patterns by using actuators/sensors that controls the thin film's thickness
- Design a control algorithm that can be achieved **in real time** making the implementation tractable for industrial control system problems.

# Case 0: KSE without feedback control, $\nu < 1$

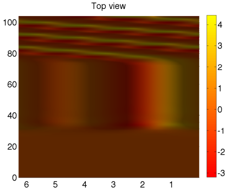


- Case $(\nu = 4/15 < 1)$ : experimentally observed that a thin film flowing in an inclined surface exhibits unwanted wavy fluctuations.
- At around time $t = 32$ a pattern starts to evolve.
- Main goal: [Christofides et al [2001+], Ahuja[2009]]. A control strategy to suppress the undesirable occurrences of these wavy patterns by using actuators/sensors that controls the thin film's thickness
- Design a control algorithm that can be achieved **in real time** making the implementation tractable for industrial control system problems.

# Example of Approximate Interpolants

**Finite volume elements**

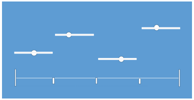

$$I_h(\varphi) = \sum_{j=1}^{N} \bar{\varphi}_k \, \chi_{J_k}(x),$$

**Approximate interpolant based on nodal values**

$$I_h(\varphi) = \sum_{k=1}^{N} \varphi(x_k) \, \chi_{J_k}(x),$$

**Projection onto Fourier modes as approximate interpolant**

$$I_h(u) = \sum_{k=1}^{m} a_k \cos kx + \sum_{k=1}^{m} b_k \sin kx, \quad h = \frac{L}{N}, \qquad (14)$$

where the Fourier coefficients are given by
$a_k = \frac{2}{L} \int_0^L u(x) \cos kx \, dx, \quad b_k = \frac{2}{L} \int_0^L u(x) \sin kx \, dx.$

# KSE with Feedback control

Feedback control system for the KSE to stabilize the steady state solution $\mathbf{v} = 0$

$$\frac{\partial u}{\partial t} = -\frac{\partial^2 u}{\partial x^2} - \nu \frac{\partial^4 u}{\partial x^4} - u\frac{\partial u}{\partial x} - \mu\, I_h(u), \quad x \in [0, 2\pi] \tag{15}$$

subject to the periodic boundary conditions, and initial condition $u(x,0) = u_0(x)$, with $\int_0^{2\pi} u(x,0)\, dx = 0$, where the interpolant operator $I_h$ acting on $u$ can be defined as a general interpolant satisfying certain properties.

# Terms

- $\frac{\partial^2 u}{\partial x^2}$ - responsible for internal destabilizing of the system
- $\frac{\partial^4 u}{\partial x^4}$ - responsible for dissipating energy and stabilizes the system.
- Together, $\frac{\partial^2 u}{\partial x^2}, \nu\frac{\partial^4 u}{\partial x^4}$ destabilizes the low modes (large scales) and stabilizes the high modes (small scales) with the positive constant $\nu$ as the stabilizing parameter.
- $u\frac{\partial u}{\partial x}$ transfers energy from low modes to high modes.
- $-\mu I_h(u)$ - responsible for stabilizing the low unstable modes, i.e. neutralizes the instability caused by $u_{xx}$
- Convergence to reference solution: technical conditions on the interpolant operator and $\mu$.

# Terms

- $\frac{\partial^2 u}{\partial x^2}$ - responsible for internal destabilizing of the system
- $\frac{\partial^4 u}{\partial x^4}$ - responsible for dissipating energy and stabilizes the system.
- Together, $\frac{\partial^2 u}{\partial x^2}, \nu \frac{\partial^4 u}{\partial x^4}$ destabilizes the low modes (large scales) and stabilizes the high modes (small scales) with the positive constant $\nu$ as the stabilizing parameter.
- $u \frac{\partial u}{\partial x}$ transfers energy from low modes to high modes.
- $-\mu I_h(u)$ - responsible for stabilizing the low unstable modes, i.e. neutralizes the instability caused by $u_{xx}$
- Convergence to reference solution: technical conditions on the interpolant operator and $\mu$.

# Numerical Results

| Case | # Actuators | $\mu$ | $\nu$ | $[0, L]$ | $[t_0, t_f]$ | $t_c$ | $N$ | $M$ |
|---|---|---|---|---|---|---|---|---|
| 0a | 0 | 0 | 1.1 | $[0, 2\pi]$ | [0, 200] | 0 | 128 | 1600 |
| 0b | 0 | 0 | 4/15 | $[0, 2\pi]$ | [0, 200] | 0 | 128 | 1600 |
| 1 | 0 | 20 | 4/15 | $[0, 2\pi]$ | [0, 200] | 0 | 128 | 1600 |
| 2a | 4 | 10 | 4/20 | $[0, 2\pi]$ | [0, 200] | 0 | 128 | 1600 |
| 2b | 4 | 10 | 4/20 | $[0, 2\pi]$ | [0, 200] | 15 | 128 | 1600 |
| 3 | 4 | 10 | 4/15 | $[0, 2\pi]$ | [0, 200] | 40 | 128 | 1600 |

Table: Model parameters and discretization parameters for the un-controlled and controlled 1D Kuramoto-Sivashinksy equations

# Case 2a: Controlled KSE with Finite Volume Elements. Control turned on at $t = t_c = 0$

- Initial condition:

$$u_0(x) = \left(2.5/\sqrt{5}\right) \sum_{n=1}^{5} (\sin(nx - n\pi) + \cos(nx - n\pi)\,.$$

- Number of controls: $NC = 4$ which is proportional to the number of unstable modes.
- Observe the closed-loop profile showing exponential stabilization of the $u(x,t) = 0$ steady state solution.

# Results

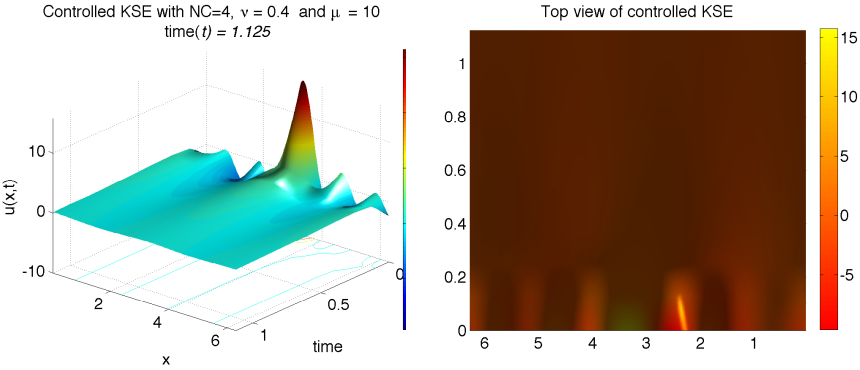


Figure: (a) Closed-loop profile showing fast stabilization of the $u(x,t) = 0$ steady state solution for $\nu = 4/20 < 1$, and with $\mu = 10$. (b) Top view profile of $u(x,t)$.

# Results

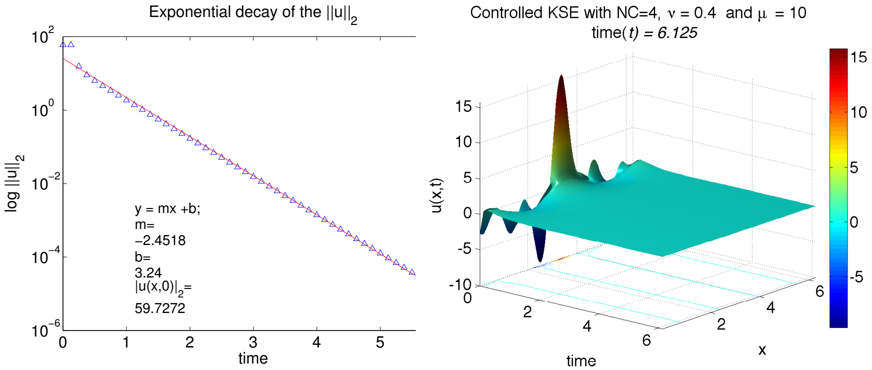


Figure: (a) Exponential decay of the $\|u\|_{L^2}$, (b) Control KSE run for longer time.

# Case 3: Controlled KSE with Finite Nodal Elements

$$\frac{\partial u}{\partial t} = -\frac{\partial^2 u}{\partial x^2} - \nu \frac{\partial^4 u}{\partial x^4} - u\frac{\partial u}{\partial x} - \mu \sum_{k=1}^{N} u(x_k^*)\, \chi_{j_k}(x). \qquad (16)$$

- $u_0 = 1e^{-10}\cos x(1+\sin x)$,
- number of controllers $NC = 4$
- relaxation parameter $\mu = 2$ which is turned on at $t_c = 40$,
- the film height starts to destabilize around $t = 32$ and then once feedback control is turned on at $t_c = 40$ it stabilizes exponentially to zero again.

# Results

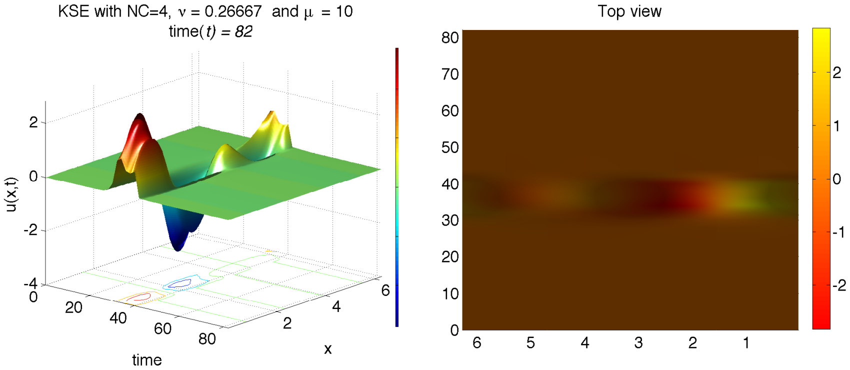


Figure: (a) $u_0 = 1e^{-10} \cos x(1 + \sin x)$, the film height starts to destabilize around $t = 32$ and then once feedback control is turned on at $t_c = 40$ it stabilizes to zero again. (b) A top view of the controlled profile.

# Predictive control of catalytic rod with or without uncertainty variables

- Catalytic rod example (Christofides).
- long thin rod in a reactor where a pure species $A$ is fed into the system and a catalytic reaction of the form

$$A \rightarrow B$$

  takes place on the rod.
- The reaction is exothermic, needs a cooling medium in contact with the rod to reduce temperature.

# Predictive control of catalytic rod with or without uncertainty variables

$u(x,t)$ - dimensionless temperature in the reactor

$$\frac{\partial u}{\partial t} = \frac{\partial^2 u}{\partial x^2} + \beta_T e^{-\frac{\gamma}{1+u}} + \beta_U \left(b(x)q(t) - u\right) - \beta_T e^{-\gamma}, \qquad (17)$$

subject to BCs:

$$u(0,t) = 0, \quad u(\pi,t) = 0,$$

- $\beta_T$ - dimensionless heat of reaction,
- $\gamma$ - dimensionless activation energy,
- $\beta_U$ - dimensionless heat transfer coefficient, and
- $q(t)$ - the manipulated input (supplied but the cooling medium),
- $b(x)$ - the actuator distribution shape function set to $b(x) = \sqrt{\frac{2}{\pi}}\sin(x)$ to supply maximum cooling in the middle of the rod.

# Predictive control of catalytic rod with or without uncertainty variables

$u(x,t)$ - dimensionless temperature in the reactor

$$\frac{\partial u}{\partial t} = \frac{\partial^2 u}{\partial x^2} + \beta_T e^{-\frac{\gamma}{1+u}} + \beta_U \left( b(x)q(t) - u \right) - \beta_T e^{-\gamma}, \qquad (17)$$

subject to BCs:

$$u(0,t) = 0, \quad u(\pi,t) = 0,$$

- $\beta_T$ - dimensionless heat of reaction,
- $\gamma$ - dimensionless activation energy,
- $\beta_U$ - dimensionless heat transfer coefficient, and
- $q(t)$ - the manipulated input (supplied but the cooling medium),
- $b(x)$ - the actuator distribution shape function set to $b(x) = \sqrt{\frac{2}{\pi}} \sin(x)$ to supply maximum cooling in the middle of the rod.

# Case 1: Uncontrolled catalytic rod

For the typical values of the model parameters,

$$\beta_T = 50, \quad \beta_U = 2, \quad \gamma = 4, \tag{18}$$

the steady state solution $u(x, t) = 0$ is unstable.

- For a small perturbation near zero, the temperature evolves to another stable steady state where the temperature profile has a hot-spot in the middle.
- For the given catalytic rod problem parameters given in (18), we have one unstable mode

# Results

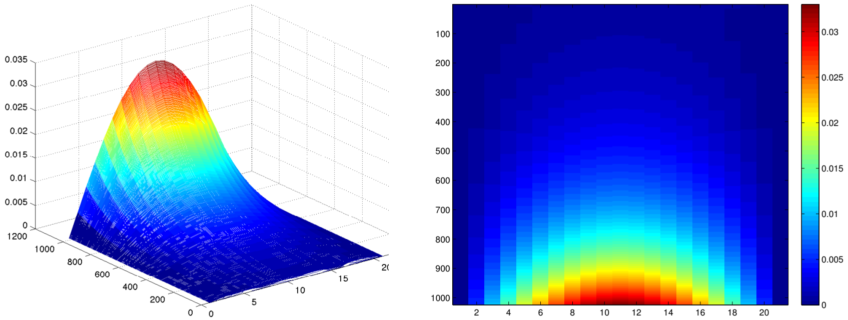


Figure: (a) Open-loop profile showing instability of the $u(x,t) = 0$ steady state solution. (b) Top-view of $u(x,t)$.

# Case 2: Controlled catalytic rod

$$\frac{\partial u}{\partial t} = \frac{\partial^2 u}{\partial x^2} + \beta_T e^{-\frac{\gamma}{1+u}} + \beta_U \left( -\mu I_h(u) - u \right) - \beta_T e^{-\gamma}. \qquad (19)$$

- We put one actuator in the middle of the rod at $x = \pi/2$.
- And our interpolant $I(u) = \bar{u}\,\chi_{[0,\pi]}(x)$, $\bar{u}$ is the spatial average of $u(x)$ in the interval $[0, \pi]$ at time $t - \Delta t$.
- We run the simulation with feedback control with initial condition, $u_0(x) = 1e^{-3}\sin(2x)$.
- We observed that both presents stabilization of the trivial steady state solution.

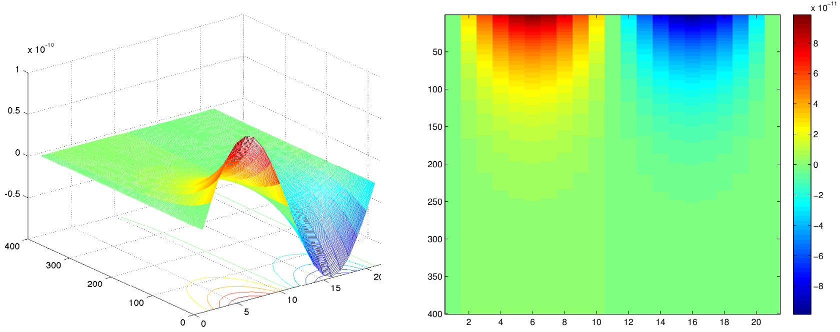


Figure: (a) Open-loop profile showing initial instability of the $u(x,t) = 0$ steady state solution and eventual stability. (b) Top-view.

# Case 3: Application to catalytic rod with uncertainty

- Catalytic rod example, assume that the heat of the reaction is unknown and varies with time.
- Goal: Stabilize the rod temperature in the presence of time-varying uncertainty in the dimensionless heat of the reaction parameter $\beta_T$.
- The location of the actuator is at $x = \pi/2$.
- Conclusion: In the presence of the uncertainty in some model parameters values, the control algorithm is able to compensate for the uncertainty.
- The result on the bounds for $u$ depends on the size of the error in the measurements.

# Case 3: Application to catalytic rod with uncertainty

- Catalytic rod example, assume that the heat of the reaction is unknown and varies with time.
- Goal: Stabilize the rod temperature in the presence of time-varying uncertainty in the dimensionless heat of the reaction parameter $\beta_T$.
- The location of the actuator is at $x = \pi/2$.
- Conclusion: In the presence of the uncertainty in some model parameters values, the control algorithm is able to compensate for the uncertainty.
- The result on the bounds for $u$ depends on the size of the error in the measurements.

# Results

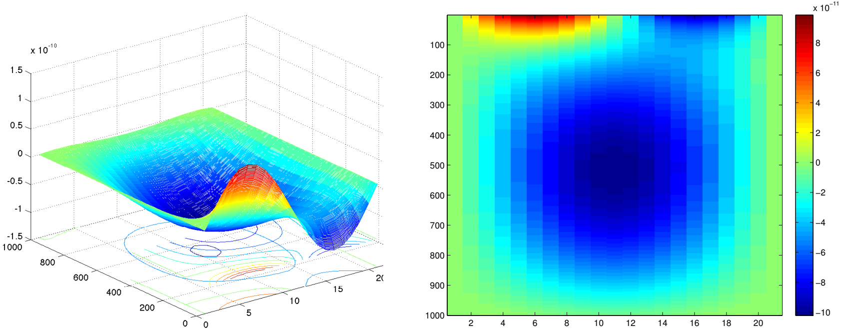


Figure: (a) Open-loop profile showing instability of the $u(x,t) = 0$ steady state solution. (b) Top-view.

# Case 4: Nodal case, sensors, controllers different

- Observables are the values of the solutions $u(\overline{x}_k)$, at the points $\overline{x}_k \in J_k = [(k-1)\frac{L}{N}, k\frac{L}{N}]$, $k = 1, ..., N$,
- Feedback controllers are at some points $x_k \in J_k$, $x_k$ is not necessarily the same as $\overline{x}_k$.
- That is the measurements are made at $\overline{x}_k$, while the feedback controllers are at $x_k$, for $k = 1, 2..., N$.

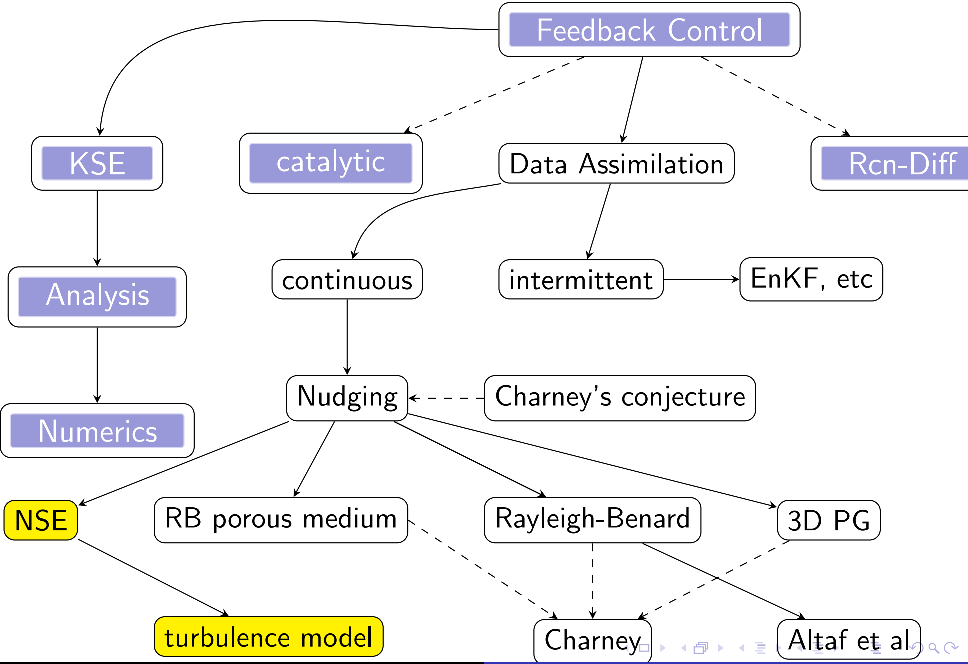
Feedback Control
KSE
catalytic
Data Assimilation
Rcn-Diff
Analysis
continuous
intermittent
EnKF, etc
Numerics
Nudging
Charney's conjecture
NSE
RB porous medium
Rayleigh-Benard
3D PG
turbulence model
Charney
Altaf et al

# Applications to other models

**[Kalantarov-Titi]** established rigorous analytic results concerning similar feedback control algorithms for the Navier-Stokes equations, Navier-Stokes-Voigt, nonlinear damped wave equations, etc....

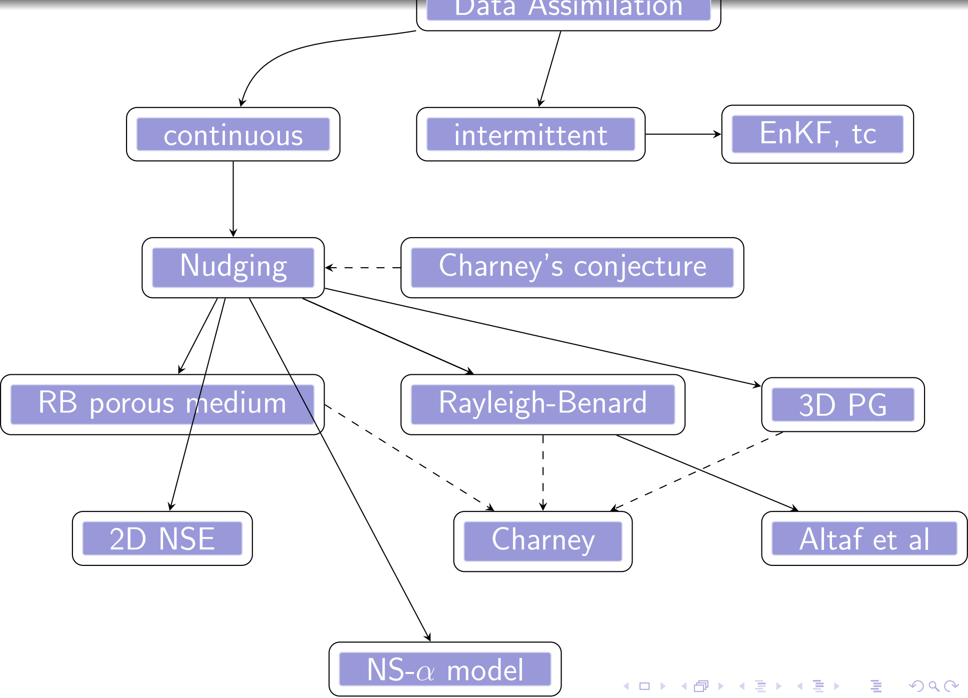
Data Assimilation
continuous
intermittent
EnKF, tc
Nudging
Charney's conjecture
RB porous medium
Rayleigh-Benard
3D PG
2D NSE
Charney
Altaf et al
NS-$\alpha$ model

Suppose that $u(t)$ represents a solution of some dissipative dynamical system governed by an evolution equation of the type

$$\frac{du}{dt} = F(u), \tag{20}$$

where the initial data $u(0) = u_0$ is **missing**.

Let $I_h(u(t))$ - an interpolant operator based on the observational measurements of this system at a coarse spatial resolution of size $h$, for $t \in [0, T]$.

DA Algorithm: [Azouani-Olson-Titi 2013] - construct an approximate solution $v(t)$ that satisfies the equations

$$\frac{dv}{dt} = F(v) - \mu(I_h(v) - I_h(u)), \tag{21a}$$

$$v(0) = v_0, \tag{21b}$$

where $\mu > 0$ is a relaxation (nudging) parameter and $v_0$ is taken to be an arbitrary initial data.

If system (21) is globally well-posed and $I_h(v)$ converge to $I_h(u)$ in time, then one recovers the reference $u(x, t)$ from the approximate solution $v(x, t)$. For large enough time $T > 0$, the solution $v(T)$ can be used as initial condition to (21) .

# General Form - Data Assimilation - Newtonian Relaxation

Suppose that $u(t)$ represents a solution of some dissipative dynamical system governed by an evolution equation of the type

$$\frac{du}{dt} = F(u), \tag{20}$$

where the initial data $u(0) = u_0$ is **missing**.

Let $I_h(u(t))$ - an interpolant operator based on the observational measurements of this system at a coarse spatial resolution of size $h$, for $t \in [0, T]$.

DA Algorithm: [Azouani-Olson-Titi 2013] - construct an approximate solution $v(t)$ that satisfies the equations

$$\frac{dv}{dt} = F(v) - \mu(I_h(v) - I_h(u)), \tag{21a}$$

$$v(0) = v_0, \tag{21b}$$

where $\mu > 0$ is a relaxation (nudging) parameter and $v_0$ is taken to be an arbitrary initial data.

If system (21) is globally well-posed and $I_h(v)$ converge to $I_h(u)$ in time, then one recovers the reference $u(x,t)$ from the approximate solution $v(x,t)$. For large enough time $T > 0$, the solution $v(T)$ can be used as initial condition to (21) .

# General Form - Data Assimilation - Newtonian Relaxation

Suppose that $u(t)$ represents a solution of some dissipative dynamical system governed by an evolution equation of the type

$$\frac{du}{dt} = F(u), \tag{20}$$

where the initial data $u(0) = u_0$ is **missing**.

Let $I_h(u(t))$ - an interpolant operator based on the observational measurements of this system at a coarse spatial resolution of size $h$, for $t \in [0, T]$.

DA Algorithm: [Azouani-Olson-Titi 2013] - construct an approximate solution $v(t)$ that satisfies the equations

$$\frac{dv}{dt} = F(v) - \mu(I_h(v) - I_h(u)), \tag{21a}$$

$$v(0) = v_0, \tag{21b}$$

where $\mu > 0$ is a relaxation (nudging) parameter and $v_0$ is taken to be an arbitrary initial data.

If system (21) is globally well-posed and $I_h(v)$ converge to $I_h(u)$ in time, then one recovers the reference $u(x, t)$ from the approximate solution $v(x, t)$. For large enough time $T > 0$, the solution $v(T)$ can be used as initial condition to (21) .

# General Form - Data Assimilation - Newtonian Relaxation

Suppose that $u(t)$ represents a solution of some dissipative dynamical system governed by an evolution equation of the type

$$\frac{du}{dt} = F(u), \tag{20}$$

where the initial data $u(0) = u_0$ is **missing**.

Let $I_h(u(t))$ - an interpolant operator based on the observational measurements of this system at a coarse spatial resolution of size $h$, for $t \in [0, T]$.

DA Algorithm: [Azouani-Olson-Titi 2013] - construct an approximate solution $v(t)$ that satisfies the equations

$$\frac{dv}{dt} = F(v) - \mu(I_h(v) - I_h(u)), \tag{21a}$$

$$v(0) = v_0, \tag{21b}$$

where $\mu > 0$ is a relaxation (nudging) parameter and $v_0$ is taken to be an arbitrary initial data.

If system (21) is globally well-posed and $I_h(v)$ converge to $I_h(u)$ in time, then one recovers the reference $u(x,t)$ from the approximate solution $v(x,t)$. For large enough time $T > 0$, the solution $v(T)$ can be used as initial condition to (21) .

# General Form - Data Assimilation - Newtonian Relaxation

Suppose that $u(t)$ represents a solution of some dissipative dynamical system governed by an evolution equation of the type

$$\frac{du}{dt} = F(u), \tag{20}$$

where the initial data $u(0) = u_0$ is **missing**.

Let $I_h(u(t))$ - an interpolant operator based on the observational measurements of this system at a coarse spatial resolution of size $h$, for $t \in [0, T]$.

DA Algorithm: [Azouani-Olson-Titi 2013] - construct an approximate solution $v(t)$ that satisfies the equations

$$\frac{dv}{dt} = F(v) - \mu(I_h(v) - I_h(u)), \tag{21a}$$

$$v(0) = v_0, \tag{21b}$$

where $\mu > 0$ is a relaxation (nudging) parameter and $v_0$ is taken to be an arbitrary initial data.

If system (21) is globally well-posed and $I_h(v)$ converge to $I_h(u)$ in time, then one recovers the reference $u(x, t)$ from the approximate solution $v(x, t)$. For large enough time $T > 0$, the solution $v(T)$ can be used as initial condition to (21) .

# General Form - Data Assimilation - Newtonian Relaxation

Suppose that $u(t)$ represents a solution of some dissipative dynamical system governed by an evolution equation of the type

$$\frac{du}{dt} = F(u), \tag{20}$$

where the initial data $u(0) = u_0$ is **missing**.

Let $I_h(u(t))$ - an interpolant operator based on the observational measurements of this system at a coarse spatial resolution of size $h$, for $t \in [0, T]$.

DA Algorithm: [Azouani-Olson-Titi 2013] - construct an approximate solution $v(t)$ that satisfies the equations

$$\frac{dv}{dt} = F(v) - \mu(I_h(v) - I_h(u)), \tag{21a}$$

$$v(0) = v_0, \tag{21b}$$

where $\mu > 0$ is a relaxation (nudging) parameter and $v_0$ is taken to be an arbitrary initial data.

If system (21) is globally well-posed and $I_h(v)$ converge to $I_h(u)$ in time, then one recovers the reference $u(x, t)$ from the approximate solution $v(x, t)$. For large enough time $T > 0$, the solution $v(T)$ can be used as initial condition to (21) .

# Basic concepts

- Added to the prognostic equation a term that nudges the solution towards observations.
- If nudging parameter $\mu$ is too big then solution converges towards observation points too fast, the dynamics do not have time to adjust – leading to the creation of spurious spill over effects.
- If the nudging parameter $\mu$ is too small, the errors in the model and measurements can grow too much before the nudging becomes effective.
- Hokes and Anthes [1976] the relaxation parameter should be chosen so that the nudging term in similar in magnitude to the less dominant terms.

# Numerical weather prediction (NWP)

- NWP - an IVP where equations for geophysical fluid dynamics are integrated forward in time from a set of initial values.
  - needs accuracy of model
  - accuracy of initial conditions
  - well-posedness
- Difficulties: data collected such as temperature and velocity measurements are usually sparse.
- Data assimilation is a proper combination of model + observations $\rightarrow$ accurate initial conditions. [survey: Dowey1992].
- Two categories: **Continuous** (insert data as received) vs. **Intermittent** (screens for bad meteorological data then after **analysis** data are assimilated intermittently at specified intervals)

# Numerical weather prediction (NWP)

- NWP - an IVP where equations for geophysical fluid dynamics are integrated forward in time from a set of initial values.
  - needs accuracy of model
  - accuracy of initial conditions
  - well-posedness
- Difficulties: data collected such as temperature and velocity measurements are usually sparse.
- Data assimilation is a proper combination of model + observations → accurate initial conditions. [survey: Dowey1992].
- Two categories: **Continuous** (insert data as received) vs. **Intermittent** (screens for bad meteorological data then after **analysis** data are assimilated intermittently at specified intervals)

# Charney 1954

**1954** - Use of Primitive equation of motion for NWP.
**Observations:**

- (obstacle) "initial values of wind and pressure cannot as a rule be prescribed independently with sufficient accuracy"
- " initial inaccuracies gives rise to spurious inertio-gravitational oscillations that obscure meteorological significant motions."
- (how to overcome)" accurate initial winds can be determine from pressure field alone, and that if this is done intertio-gravitational oscillations will not arise"

# Charney et al 1969

- Charney, Halem, Jastrom [1969] - Use of incomplete historical data to infer the present state of the atmosphere - launch of temperature sounding satellite. (See also, Smagarinsky 1970, Rutherford 1972, Morel and Telegrand 1974)
  - If it is possible to obtain large-scale wind field from temperatures alone then NWP would be substantially advanced.
  - Mintz-Arakawa global circulation model (predicts winds and temperatures at 800 and 400 mb and pressure at sea level.)
- Jastrom, Halem [1970] - Used **Direct insertion method** - observation simply replaced the model forecast at model grid point nearest the observation location. (limited success).
  - gives rise to shocks.
  - when applied to primitive equation model an imbalance between the mass and wind fields generates non physical oscillations when the model integration is resumed.
  - model attempting to restore the dynamic balance [Bengston 1975].

# Charney et al 1969

- Charney, Halem, Jastrom [1969] - Use of incomplete historical data to infer the present state of the atmosphere - launch of temperature sounding satellite. (See also, Smagarinsky 1970, Rutherford 1972, Morel and Telegrand 1974)
  - If it is possible to obtain large-scale wind field from temperatures alone then NWP would be substantially advanced.
  - Mintz-Arakawa global circulation model (predicts winds and temperatures at 800 and 400 mb and pressure at sea level.)
- Jastrom, Halem [1970] - Used **Direct insertion method** - observation simply replaced the model forecast at model grid point nearest the observation location. (limited success).
  - gives rise to shocks.
  - when applied to primitive equation model an imbalance between the mass and wind fields generates non physical oscillations when the model integration is resumed.
  - model attempting to restore the dynamic balance [Bengston 1975].

- Data assimilation algorithm based on feedback control theory.
- Types of applications we've analysized motivated by Charney's conjecture. Our analytical results support Charney's conjecture that temperature observations are enough to determine all the dynamical state of the system for certain models.

# Azouani-Olson-Titi [2013]

Approximate solution, $U(t, x, y)$ for the reference solution $u(t, x, y)$ to the 2D NSE, for $t \in [0, T]$ is given by

$$\frac{\partial U_1}{\partial t} - \nu \Delta U_1 + U_1 \partial_x U_1 + U_2 \partial_y U_1 + \partial_x P = f_1 - \mu(I_h(U_1) - I_h(u_1)),$$
$$\frac{\partial U_2}{\partial t} - \nu \Delta U_2 + U_1 \partial_x U_2 + U_2 \partial_y U_2 + \partial_y P = f_2 - \mu(I_h(U_2) - I_h(u_2)),$$
$$\partial_x U_1 + \partial_y U_2 = 0,$$
$$U_1(0, x, y) = U_1^0(x, y), \quad U_2(0, x, y) = U_2^0(x, y).$$

$P$ is the approximate pressure. A choice for $U_1^0$ and $U_2^0$ is arbitrary. $\mu$ is a positive nudging parameter, which relaxes (nudges) the coarse spatial scales of $U_2$ toward those of the observed data $I_h(u_1)$, $I_h(u_2)$.

Approximate solution, $U(t, x, y)$ for the reference solution $u(t, x, y)$ to the 2D NSE, for $t \in [0, T]$ is given by

$$\frac{\partial U_1}{\partial t} - \nu \Delta U_1 + U_1 \partial_x U_1 + U_2 \partial_y U_1 + \partial_x P = f_1 - \mu(I_h(U_1) - I_h(u_1)),$$
$$\frac{\partial U_2}{\partial t} - \nu \Delta U_2 + U_1 \partial_x U_2 + U_2 \partial_y U_2 + \partial_y P = f_2 - \mu(I_h(U_2) - I_h(u_2)),$$
$$\partial_x U_1 + \partial_y U_2 = 0,$$
$$U_1(0, x, y) = U_1^0(x, y), \quad U_2(0, x, y) = U_2^0(x, y).$$

$P$ is the approximate pressure. A choice for $U_1^0$ and $U_2^0$ is arbitrary. $\mu$ is a positive nudging parameter, which relaxes (nudges) the coarse spatial scales of $U_2$ toward those of the observed data $I_h(u_1)$, $I_h(u_2)$.

# Gesho, Olson, Titi [2015]

Figure 3: The error $\|u(t) - v(t)\|_V$ versus $t$ for $h = 0.6981$.

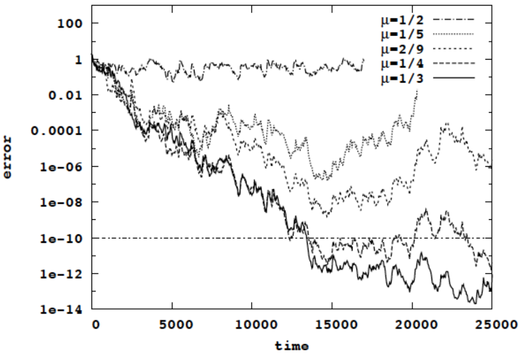


$\mu = 1/3$

# The 2D Bénard convection problem

$$\frac{\partial u}{\partial t} - \nu \Delta u + (u \cdot \nabla) u + \nabla p = \theta \mathbf{e}_2, \tag{23a}$$

$$\frac{\partial \theta}{\partial t} - \kappa \Delta \theta + (u \cdot \nabla) \theta - u \cdot \mathbf{e}_2 = 0, \tag{23b}$$

$$\nabla \cdot u = 0, \tag{23c}$$

$$u(0,x,y) = u_0(x,y), \quad \theta(0,x,y) = \theta_0(x,y), \tag{23d}$$

with appropriate boundary conditions. Farhat-Jolly-Titi[2015]

$$\frac{\partial U}{\partial t} - \nu \Delta U + (U \cdot \nabla) U + \nabla P = \eta \mathbf{e}_2 - \mu (I_h(U) - I_h(u)), \tag{24a}$$

$$\frac{\partial \eta}{\partial t} - \kappa \Delta \eta + (U \cdot \nabla) \eta - U \cdot \mathbf{e}_2 = 0, \tag{24b}$$

$$\nabla \cdot U = 0, \tag{24c}$$

$$U(0,x,y) = U_0(x,y), \quad \eta(0,x,y) = \eta_0(x,y), \tag{24d}$$

Can we design a DA algorithm for the Bénard convection model, based on temperature measurements only.

# The 2D Bénard convection problem

$$\frac{\partial u}{\partial t} - \nu \Delta u + (u \cdot \nabla) u + \nabla p = \theta \mathbf{e}_2, \tag{23a}$$

$$\frac{\partial \theta}{\partial t} - \kappa \Delta \theta + (u \cdot \nabla) \theta - u \cdot \mathbf{e}_2 = 0, \tag{23b}$$

$$\nabla \cdot u = 0, \tag{23c}$$

$$u(0, x, y) = u_0(x, y), \quad \theta(0, x, y) = \theta_0(x, y), \tag{23d}$$

with appropriate boundary conditions. **Farhat-Jolly-Titi[2015]**

$$\frac{\partial U}{\partial t} - \nu \Delta U + (U \cdot \nabla) U + \nabla P = \eta \mathbf{e}_2 - \mu (I_h(U) - I_h(u)), \tag{24a}$$

$$\frac{\partial \eta}{\partial t} - \kappa \Delta \eta + (U \cdot \nabla) \eta - U \cdot \mathbf{e}_2 = 0, \tag{24b}$$

$$\nabla \cdot U = 0, \tag{24c}$$

$$U(0, x, y) = U_0(x, y), \quad \eta(0, x, y) = \eta_0(x, y), \tag{24d}$$

Can we design a DA algorithm for the Bénard convection model, based on temperature measurements only.

# The 2D Bénard convection problem

$$\frac{\partial u}{\partial t} - \nu\Delta u + (u\cdot\nabla)u + \nabla p = \theta \mathbf{e}_2, \tag{23a}$$
$$\frac{\partial \theta}{\partial t} - \kappa\Delta\theta + (u\cdot\nabla)\theta - u\cdot\mathbf{e}_2 = 0, \tag{23b}$$
$$\nabla\cdot u = 0, \tag{23c}$$
$$u(0,x,y) = u_0(x,y), \quad \theta(0,x,y) = \theta_0(x,y), \tag{23d}$$

with appropriate boundary conditions. **Farhat-Jolly-Titi[2015]**

$$\frac{\partial U}{\partial t} - \nu\Delta U + (U\cdot\nabla)U + \nabla P = \eta \mathbf{e}_2 - \mu(I_h(U) - I_h(u)), \tag{24a}$$
$$\frac{\partial \eta}{\partial t} - \kappa\Delta\eta + (U\cdot\nabla)\eta - U\cdot\mathbf{e}_2 = 0, \tag{24b}$$
$$\nabla\cdot U = 0, \tag{24c}$$
$$U(0,x,y) = U_0(x,y), \quad \eta(0,x,y) = \eta_0(x,y), \tag{24d}$$

Can we design a DA algorithm for the Bénard convection model, based on temperature measurements only

Can we design a DA algorithm for the Bénard convection model, based on temperature measurements only?

# Continuous Data Assimilation (CDA) for 2D Bénard

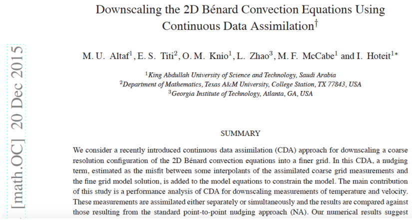

[math.OC] 20 Dec 2015

Downscaling the 2D Bénard Convection Equations Using Continuous Data Assimilation†

M. U. Altaf[1], E. S. Titi[2], O. M. Knio[1], L. Zhao[3], M. F. McCabe[1] and I. Hoteit[1*]

[1] King Abdullah University of Science and Technology, Saudi Arabia
[2] Department of Mathematics, Texas A&M University, College Station, TX 77843, USA
[3] Georgia Institute of Technology, Atlanta, GA, USA

SUMMARY

We consider a recently introduced continuous data assimilation (CDA) approach for downscaling a coarse resolution configuration of the 2D Bénard convection equations into a finer grid. In this CDA, a nudging term, estimated as the misfit between some interpolants of the assimilated coarse grid measurements and the fine grid model solution, is added to the model equations to constrain the model. The main contribution of this study is a performance analysis of CDA for downscaling measurements of temperature and velocity. These measurements are assimilated either separately or simultaneously and the results are compared against those resulting from the standard point-to-point nudging approach (NA). Our numerical results suggest

Performance Analysis of CDA when downscaling measurements

- of temperature and velocity ✓
- of velocity alone ✓
- of temperature alone $X$

When assimilating only temperature with CDA, the temperature converges exponentially but the velocity does not converge. Eg. Assimilation starts from an initial shear flow. In this case, velocity field suffers from large errors

Figure: (a) Numerical Study of Data Assimilation for 2D Bénard Problem by Altaf et al. Results are compared to point to point nudging approach.

# Approximate Solution: Standard Grid Nudging Approach (NA) vs Continuous Data Assimilation (CDA)

$$\frac{\partial \boldsymbol{u}}{\partial t} - \frac{Pr}{\sqrt{Ra}} \nabla^2 \boldsymbol{u} + (\boldsymbol{u} \cdot \nabla) \boldsymbol{u} + \nabla p = \Theta \boldsymbol{e}_2 - \mu_u (I_h(\boldsymbol{u}^o) - I_h(\boldsymbol{u})),$$

$$\frac{\partial \Theta}{\partial t} - \frac{1}{\sqrt{Ra}} \nabla^2 \Theta + (\boldsymbol{u} \cdot \nabla) \Theta - \boldsymbol{u} \cdot \boldsymbol{e}_2 = -\mu_\theta (I_h(\Theta^o) - I_h(\Theta)),$$

$$\nabla \cdot \boldsymbol{u} = 0,$$

with zero initial conditions and where for example,

$$I_h(\phi)(x) = \sum_{k=1}^{N} \phi(x_k^*) \, \chi_{J_k}$$

# Farhat, Lunasin, Titi [2015]

A data assimilation algorithm for the 2D Navier-Stokes Equations utilizing measurements of only one component of the velocity field.

$$
\begin{aligned}
\frac{\partial U_1}{\partial t} - \nu \Delta U_1 + U_1 \partial_x U_1 + U_2 \partial_y U_1 + \partial_x P &= f_1, \\
\frac{\partial U_2}{\partial t} - \nu \Delta U_2 + U_1 \partial_x U_2 + U_2 \partial_y U_2 + \partial_y P &= f_2 - \mu (I_h(U_2) - I_h(u_2)), \\
\partial_x U_1 + \partial_y U_2 &= 0, \\
U_1(0,x,y) = U_1^0(x,y), \quad U_2(0,x,y) &= U_2^0(x,y).
\end{aligned}
$$

# Farhat, Lunasin, Titi [2016]

Data assimilation algorithm for a two-dimensional Bénard convection problem: two-dimensional Boussinesq system of a layer of incompressible fluid between two solid horizontal walls, with no-normal flow and stress free boundary condition on the walls, and fluid is heated from the bottom and cooled from the top.

We incorporate the observables as a feedback (nudging) term in the evolution equation of the horizontal velocity.

# 3D Bénard Problem in Porous Medium

Fluid flow through a porous media such as flow within and between rock layers.

$$\gamma \frac{\partial u}{\partial t} + u + \nabla p = Ra\,\theta \hat{k}, \tag{26a}$$

$$\frac{\partial \theta}{\partial t} - \Delta\theta + (u \cdot \nabla)\theta - u \cdot \hat{k} = 0, \tag{26b}$$

$$\nabla \cdot u = 0, \tag{26c}$$

$$u(0; x, y, z) = u^0(x, y, z), \quad \theta(0; x, y, z) = \theta^0(x, y, z), \tag{26d}$$

subject to the boundary conditions:

$$\theta(t; x, y, 0) = \theta(t; x, y, 1) = 0, \tag{26e}$$

$$\frac{\partial \theta}{\partial x}(t; 0, y, z) = \frac{\partial \theta}{\partial x}(t; L, y, z) = \frac{\partial \theta}{\partial y}(t; x, 0, z) = \frac{\partial \theta}{\partial y}(t; x, l, z) = 0, \tag{26f}$$

$$u \cdot \hat{n} = 0, \quad \text{on } \partial\Omega. \tag{26g}$$

# Data Assimilation for 3D Bénard Problem in Porous Medium employing temperature measurements

Our algorithm: (Farhat, Lunasin, Titi 2015)

$$\gamma \frac{\partial v}{\partial t} + v + \nabla q = Ra\, \eta \hat{k}, \tag{27a}$$

$$\frac{\partial \eta}{\partial t} - \Delta \eta + (v \cdot \nabla)\eta - v \cdot \hat{k} = -\mu(I_h(\eta) - I_h(\theta)), \tag{27b}$$

$$\nabla \cdot v = 0, \tag{27c}$$

$$v(0; x, y, z) = v^0(x, y, z), \quad \eta(0; x, y, z) = \eta^0(x, y, z), \tag{27d}$$

subject to the appropriate boundary conditions.

# Planetary Geostrophic equations

Planetary scale ocean circulation model

$$\nabla p + f\vec{k} \times u + \epsilon L_1 u = 0, \quad (0.1a)$$
$$\partial_z p + T = 0, \quad (0.1b)$$
$$\nabla \cdot u + \partial_z w = 0, \quad (0.1c)$$
$$\partial_t T + u \cdot \nabla T, + w\partial_z T + L_2 T = Q. \quad (0.1d)$$

For simplicity, we focus in the case of ocean dynamics and consider the above system in the domain

$$\Omega = M \times (-h, 0) \subset \mathbb{R}^3,$$

where $M$ is a bounded smooth domain in $\mathbb{R}^2$, or the square $M = (0,1) \times (0,1)$. Here $u = (u_1, u_2)$ and $(u_1, u_2, w)$ is the velocity field, $T$ is the temperature, and $p$ is the pressure. $f = f_0(\beta + y)$ is the Coriolis parameter, $Q$ is a heat source, and $\epsilon$

is a positive constant. The operators $L_1$ and $L_2$ are given by

$$L_1 = -A_h\Delta - A_v\partial_z^2,$$
$$L_2 = -K_h\Delta - K_v\partial_z^2,$$

where $A_h$ and $A_v$ are positive molecular viscosities, and $K_h$ and $K_v$ are positive conductivity constants. We set $\nabla p = (\partial_x p, \partial_y p), \nabla \cdot u = \partial_x u_1 + \partial_y u_2$ and $\Delta = \partial_x^2 + \partial_y^2$. We denote the different parts of the boundary of $\Omega$ by:

$$\Gamma_u = \{(x,y,z) \in \Omega : z = 0\},$$
$$\Gamma_b = \{(x,y,z) \in \Omega : z = -h\},$$
$$\Gamma_s = \{(x,y,z) \in \Omega : (x,y) \in \partial M\}.$$

We equip system (0.1a)–(0.1d) with the following boundary conditions – with wind-driven on the top surface and non-slip and non-flux on the side walls and bottom

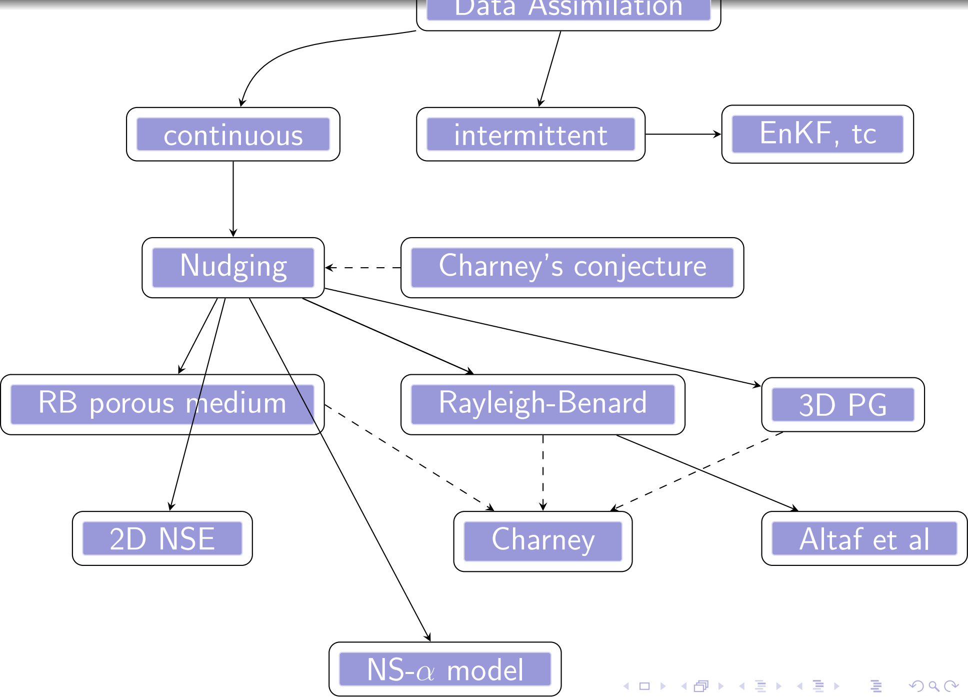
Data Assimilation
continuous
intermittent
EnKF, tc
Nudging
Charney's conjecture
RB porous medium
Rayleigh-Benard
3D PG
2D NSE
Charney
Altaf et al
NS-$\alpha$ model

# Acknowledgments

Many thanks!